

Discovery of Red-Skewed K_α iron line in Cyg X-2 with *Suzaku*

Nikolai Shaposhnikov¹, Lev Titarchuk² and Philippe Laurent³

ABSTRACT

We report on the *Suzaku* observation of neutron star low-mass X-ray binary Cygnus X-2 which reveals strong iron K_α emission line. The line profile shows a prominent red wing extending down to 4 keV. This discovery increases the number of neutron star sources where red-skewed iron lines were observed and strongly suggests that this phenomenon is common not only in black holes but also in other types of compact objects. We examine the line profile by fitting it with the model which attributes its production to the relativistic effects due to disk reflection of X-ray radiation. We also apply an alternative model where the red wing is a result of down-scattering effect of the first order with respect to electron velocity in the wind outflow. Both models describe adequately the observed line profile. However, the X-ray variability in a state similar to that in the *Suzaku* observation which we establish by analysing *RXTE* observation favors the wind origin of the line formation.

Subject headings: accretion, accretion disks —stars: neutron —X-rays: individual (Cygnus X-2) — stars:

1. Introduction

Recent discovery of red-skewed iron lines in spectra of neutron star (NS) sources Serpens X-1 (Bhattacharyya & Strohmayer 2007), 4U 1820-30 and GX 349+2 (Cackett et al. 2008, C08 hereafter) shows that the phenomenon of red-skewed lines is not restricted to black hole (BH) sources. In this Letter we report on the discovery of the red-skewed iron line profile

¹ CRESST/USRA/NASA GSFC, Astrophysics Science Division, Greenbelt MD 20771; nikolai@milkyway.gsfc.nasa.gov

²George Mason University/Center for Earth Observing and Space Research, Fairfax, VA 22030; US Naval Research Laboratory, Code 7655, Washington, DC 20375; email: Lev.Titarchuk@nrl.navy.mil; NASA GSFC, code 661, Greenbelt MD 20771, USA; email:lev@milkyway.gsfc.nasa.gov

³CEA/DSM/DAPNIA/SAP, CEA Saclay, 91191 Gif sur Yvette, France;pl Laurent@cea.fr; Laboratoire APC, 10 rue Alice Domont et Leonie Duquet, 75205 Paris Cedex 13, France

in the *Suzaku* spectrum of the NS source Cygnus X-2. This is the fourth NS source which shows red-skewed iron line profile. This indicates that red-skewed lines in NS sources may be as common as in BH sources. It is crucial to correctly identify the physical origin of the red-skewness of these lines because they can be potentially used to identify the properties of the accretion flow close to a compact object as well as to constrain the fundamental characteristics of the compact object itself.

C08 interpreted the K_α iron line profiles in terms of relativistically red-shifted emission due to reflection off the accretion disk very close to a compact object. This scenario is commonly accepted as an explanation of strongly red-skewed iron lines in BH sources (Miller 2007). The main motivation for this interpretation was the fact that the inner radius of the accretion disk, which was implied by the relativistic line model was consistent with the interpretation of the highest observed kilohertz quasi-periodic oscillation (kHz QPO) frequency in this sources as being a Keplerian frequency at this radius.

A red-skewed profile of emission lines can also be produced by repeated electron scattering in a diverging outflow as proposed by Laurent & Titarchuk (2007), see also references therein. In the framework of the wind model the fluorescent iron line K_α is formed in the partly ionized wind as a result of illumination by central source. Electron scattering of the iron K_α photons within the ionized expanding flow leads to a decrease of their energy (redshift). This photon redshift is an intrinsic property of any outflow for which divergence is positive.

We examine the red-skewed line profile observed in Cygnus X-2 both in terms of relativistic paradigm and in terms of downscattering in the wind outflow. We find that wind outflow model is able to produce the red-skewed line profile observed in the data with the fit quality similar to that shown by the relativistic reflection models. However, the requirement of a thin cold disk next to NS surface present a difficulty for relativistic reflection scenario. Timing behavior of X-ray emission from the source inferred from the Rossi X-ray Timing Explorer (*RXTE*) data further indicate that the red-skewed line formation in the wind present more natural alternative to the relativistic model.

Cyg X-2 is a low mass X-ray binary (see Lewin et al. 1995, for review) which exhibits Z-shape color-color diagram (Hasinger & van der Klis 1989). The observation of thermonuclear X-ray bursts (Smale 1998) strongly favored the nature of the compact object in Cyg X-2 as a neutron star. Titarchuk & Shaposhnikov (2002) used the *RXTE* burst data to estimate the NS mass to be about 1.4 solar masses and radius to be about 9 km. Wijnands et al. (1998) reported the simultaneous detection of twin kHz peaks at 500 and 860 Hz and highest single kHz QPO at 1007 Hz.

Description of *Suzaku* and supporting *RXTE* observations as well details of our spectral fitting are presented in §2. We discuss implications of the relativistic and wind outflow models in Cyg X-2 in §3. Discussion and conclusions follow in §4.

2. Observations and Spectral Modeling

Cyg X-2 was observed by *Suzaku* (Mitsuda et al. 2007) on May 16, 2006 for a total exposure of 39 ksec (Observation ID: 401049010). The XIS detectors operated in Burst Clock mode with 1/4 Window option to avoid effects of photon pile-up. We analyze *Suzaku* data according to guidelines given by *Suzaku* Data Analysis Guide ¹. We use the data from the foreground illuminated XIS detectors (i.e. 0, 2 and 3) from standard data products and we use canned response files. We linearly rebin XIS spectral and response data to have 512 bins. For HXD/PIN detector we also use the source spectrum from the standard products. We fit XIS and PIN spectra jointly in XSPEC using 0.6-10.0 keV range for XIS data and 15.0-30.0 range for PIN data allowing the cross-normalization factor between XIS and PIN spectra to change free. Due to large calibration uncertainties we also ignore 1.5-2.5 keV range for XIS spectrum.

For the continuum spectra we choose the sum of multicolor accretion disk (**diskbb**; Mitsuda et al. 1984) component and a Comptonized component (**comptt**; Titarchuk 1994), modified by interstellar photoelectric absorption according to Morrison & McCammon (1983). When we directly fit the data with this model we observe three distinct narrow features in the residuals (See Figure 1 panel A). First, we see a line signature at 6-7 keV, which is the primary target of our investigation. We also observe a weaker excess around 3.2 keV and a prominent line at 1 keV. The feature at 3.2 keV is probably an instrumental artifact. The line at 1 keV was reported previously from Cyg X-2 (Smale et al. 1993) and is presumably a source feature. Both features are well represented by **gaussian** shape (see residuals on panel B of Figure 1). Finally, we excluded 4.0-7.5 keV energy range where the line emission is expected to be significant and fit the spectrum again to obtain the fit quality of $\chi^2_{red} = 1.37$. The result is shown on panel C of Fig. 1.

The final best fit parameters for the continuum model are following: hydrogen column $N_H = 0.27 \pm 0.01 \times 10^{-22}$ for **wabs**; seed photons temperature $T_0 = 0.84 \pm 0.07$ keV, electron temperature $kT = 2.49 \pm 0.04$ keV, optical depth $\tau_p = 18.1 \pm 3.2$ for **comptt**, inner disk temperature $T_{in} = 1.12 \pm 0.11$ for **diskbb**. The best-fit parameters for Gaussians used to fit lines are $E_L = 1.004 \pm 0.003$ keV, $\sigma_L = 0.122 \pm 0.005$ and $E_L = 3.22 \pm 0.02$ keV,

¹http://heasarc.gsfc.nasa.gov/docs/suzaku/aehp_data_analysis.html

$\sigma_L = 0.11 \pm 0.02$. When we include iron line region (4.0-7.5 keV energy band) and fit the spectrum with the aforementioned line models these parameters change insignificantly (see Table 1). This indicates that continuum model very weakly depends on the line component

It is worth noting that the values of the continuum parameters imply that during this *Suzaku* observation Cyg X-2 was in the “high/soft” state characterized by high opacity of geometrically thin configuration. Finally, panel D shows the residuals from the same best fit model with iron region noticed in the data. The apparent line profile is broad and red-skewed. In fact, the fit using the **gaussian** line model (Model 1) produces unsatisfactory $\chi_{red}^2 = 1.47$.

We apply physically motivated models to describe this red-skewed line profile. Namely, relativistic models **diskline** (Fabian et al. 1989) and **laor** (Laor 1991) and the the wind outflow model **windline** (Laurent & Titarchuk 2007). We refer to these models as Model 2, 3 and 4 respectively. The parameters of the **laor** and **diskline** models are: the line energy E_L , inner and outer disk radius R_{in} and R_{out} , emissivity index β_L and inclination angle i_l . In modeling the data with these models R_{out} was fixed at its default value of $1000 R_G$ for **diskline** and $400 R_G$ for the **laor**. To avoid unphysical results we constrained the value of the inner radius R_{in} to be not less than $3R_G$ as dictated by the NS compactness limit (see e.g. Lattimer & Prakash 2007). The **windline** model is not in the standard set of XSPEC models and introduced as a local model during our modeling. The **windline** model calculates the line profile by means of MC simulations. The main parameters of the model are input line energy E_L , optical depth of the wind τ_w , wind electron temperature kT_w and a dimensionless wind speed v/c . For the presented study we used 10000 photons for the **windline** MC simulations. We summarize the results of our modeling and fit quality in Table 1. The resulting values of χ_{red}^2 for Models 2,3 and 4 are 1.27,1.28 and 1.22 respectively. On Figure 2 we present the unfolded spectral fit with Model 4.

We also analyze the data from two long *RXTE* observations (Obs. IDs 10066-01-01-001 and 40021-01-02-000) to demonstrate the evolution of timing properties of Cyg X-2. We extract the *RXTE*/PCA energy spectra from Standard2 data modes and we use high resolution modes to calculate power density spectra (PDS). We fit energy spectra in XSPEC with the model **wabs(comptt+diskbb+gaussian)** with **gaussian** being used to model the iron line. N_H column density was fixed at 2×10^{21} . We obtain the following best-fit values. For ObsID 10066-01-01-001, **comptt**: $T_0 = 0.79 \pm 0.6$ keV, $kT_e = 2.79 \pm 0.02$ keV, $\tau_p = 11.8 \pm 0.2$, **diskbb**: $T_{in} = 1.7 \pm 0.4$ keV, **gaussian**: $E_L = 6.61 \pm 0.03$ keV, $\sigma_L = 0.86 \pm 0.4$. For ObsID 40021-01-02-000, **comptt**: $T_0 = 1.05 \pm 0.5$ keV, $kT_e = 2.69 \pm 0.04$ keV, $\tau_p = 23 \pm 9$, **diskbb**: $T_{in} = 1.6 \pm 0.3$ keV, **gaussian**: $E_L = 6.49 \pm 0.03$ keV, $\sigma_L = 0.87 \pm 0.5$. *It is remarkable that spectral parameters for observation ID 40021-01-02-000 match closely*

those for *Suzaku* spectrum. Thus, this particular *RXTE* observation can reveal the timing properties of the source during the spectral state which is very similar to that during *Suzaku* observation when the iron line was detected. In Figure 3 we present *RXTE* energy spectra along with power spectra (PDSs) related to observations ID10066-01-01-001 (black) and ID 40021-01-02-000 (red).

3. Discussion

After detection of the red-shifted iron lines in Serp X-1, 4U 1820-30 and GX 349+2 by Bhattacharyya & Strohmayer (2007) and C08, Cyg X-2 is the fourth NS source that show strongly red-skewed line profile. This shows that red-skewed line may be as abundant in NS sources as they are in BHs (e.g. Miller 2007). C08 interpreted the lines which they observed as the evidence of relativistic distortion due to the reflection from inner disk located close to the NS surface. The main argument in the association of the line skewness with the inner disk was that the highest observed kilohertz QPO in these sources is consistent with the Keplerian frequency at the inner disk radius predicted by the line profile.

Model 2, which employs the `diskline` component to fit the iron line, predicts that in Cyg X-2 the inner disk radius at 16.8 km for NS mass of $1.4M_{\odot}$. C08 found that their values of R_{in} were consistent with inner disk radius predicted by beat-frequency model (Miller et al. 1998) from kHz QPO values. Maximum kHz QPO value observed in Cyg X-2 is 1007 kHz, which translates to 16.7 km radius if interpreted as a Keplerian frequency at the inner disk. Despite this agreement, we have to note that the interpretation of the highest kHz QPO peak as a Keplerian frequency is not unique. For example, the transition layer (TL) model treats a lower kHz QPO peak as the Keplerian frequency. (see Titarchuk 2002, and references therein). The TL model successfully describes the behavior of kHz QPOs in NS sources. According to TL QPO classification, Keplerian frequency is presented by lower kHz peak, which leads to the radius of the inner edge of 22.5 km. Beyond this radius accreting gas enters the TL to adjust its motion to the rotation of the central star. While the value of the disk inner radius given by `diskline` model for the iron line can be considered in satisfactory agreement with beat-frequency QPO model, it is hard to reconcile with the TL paradigm.

Model 3 exhibits the same statistical performance as Model 2 and provides similar physical parameters. However, we should note that the `laor` model was formulated for the extreme Kerr BH case [see Laor (1991)]. In this model the spin parameter $j = cJ/GM^2$ was assumed to be close to unity. Moderately rotating accreting NSs have spin parameters less than 0.5. The NS spin in Cyg X-2 is not exactly known but if the difference between

kHz QPO of ~ 364 Hz is taken as a spin estimate then the space-time background near Cyg X-2 should satisfy Schwarzschild metric within 10% margin of error.

The red-skewed line - kHz QPO connection is based on *highest observed* kHz QPO values. However, the duty cycle of kHz QPOs is low. As noted by C08, the most compelling evidence for the inner disk origin of the line would come from the simultaneous observation of the high kHz QPO values and red-skewed iron line. Unfortunately, simultaneous high temporal and spectral resolution observations are not currently available. In fact, we can infer the fast timing properties based on the archival *RXTE* data by matching the spectral parameters shown by *RXTE*/PCA spectrum with those observed in the *Suzaku* spectrum. We search *RXTE* archive and find that the spectrum observed for observation 40021-01-02-00 matches closely to the *Suzaku* spectrum, i.e. $\tau_p = 23 \pm 2$ and $kT_e = 2.69 \pm 0.02$. To compare this observation with the spectral state characterized by less opacity we arbitrarily choose the observation 10066-01-01-001 which is fit by `comptt` model with parameters $\tau_p = 11.8 \pm 0.2$ and $kT_e = 2.8 \pm 0.02$. In Figure 3 we show energy and power spectra for these observations. It is important to emphasize that the variability for frequencies higher than 1 Hz is strongly suppressed to a “forest”-type PDS during the *RXTE* observation for which photon spectrum closely matches the *Suzaku* spectral data. This suppression of variability can be readily explained by a smearing of a signal in the opaque wind of optical depth τ_w as the suppression factor is $\sim e^{-\tau_w}$. A higher *gaussian* equivalent width of 160 keV related to 40021-01-02-00 *RXTE* observation with respect to that of 110 eV during 10066-01-01-001 observation is another factor to support the wind-line connection.

Cyg X-2 is a Z source (Hasinger & van der Klis 1989) which are presumed to accrete at near-Eddington rates. Therefore, strong outflows are expected in these sources. In this case the red-wing of the iron line would be naturally produced in the wind/outflow configuration. This hypothesis is supported by the fact that Z sources have strong radio counterparts. Paizis et al. (2006) analysis of radio/X-ray correlation in Z and bright atoll sources that radio and Comptonized emission in these sources originate in same optically thick plasma with the temperature 2.5-3 keV near NS. The existence of the bounded configuration close to NS is also suggested by the analysis of broad band power density spectra from Cyg X-2 in the range 1.0×10^{-6} -1000 Hz by (Titarchuk, Shaposhnikov & Arefiev 2007). The strong requirement that the disk illumination be concentrated very close to its inner edge (Nandra et al 1999) in the relativistic scenario for the red-skewed line production led Reynolds & Begelman (1997) to consider the formation of fluorescent emission within the innermost stable orbit region where matter spirals into the compact object. However, as indicated by the models of Nayakshin et al. (2000), Ballantyne et al. (2001) the ionization of such a disk by the intense X-ray radiation might further invalidate some of basic assumptions associated with this interpretation. These arguments indicate that the wind/outflow paradigm, which

does not have the difficulties mentioned above, may indeed be at work as an origin of the red-skewed iron line in compact sources.

4. Conclusions

We present the analysis of the *Suzaku* spectrum from NS Cyg X-2. We discover strong K_α iron line which shows significant red-wing. This is the fourth NS source so far to show strongly distorted line profile. We analyze the line in terms of relativistic emission from the inner accretion disk and in terms of wind outflow model.

We conclude that while both model are acceptable according to the statistical criteria, the wind model appears to give more adequate explanation which does not require the accretion disk inner edge to advance close to NS surface. We also consider the line production scenarios in the context of the timing properties. In fact, we identify *RXTE* observation during which the photon spectrum is close to that during *Suzaku* observations when the red-skewed line was detected. These *RXTE* data indicate that the source fast variability is strongly suppressed, which is presumably due to smearing in a strong wind. This lack of high frequency variability weakens the red-skewed line connection with kHz QPO and strengthen its connection to a wind/outflow phenomena.

REFERENCES

- Ballantyne, D.R., Ross, R.R. & Fabian, A.C. 2001, MNRAS, 327, 10
- Bhattacharyya, S., & Strohmayer, T. E. 2007, ApJ, 664, L103
- Cackett, E. M., et al. 2008, ApJ, 674, 415
- Fabian, A. C., Rees, M. J., Stella, L., & White, N. E. 1989, MNRAS, 238, 729
- Fabian, A. C. 1995, MNRAS, 277, L11
- Hasinger, G. & van der Klis, M. 1989, A&A, 225, 79
- Laming, J.M. & Titarchuk, L. 2004, ApJ, 615, L121
- Laor, A. 1991, ApJ, 376, 90
- Lattimer, J. M., & Prakash, M. 2007, Phys. Rep., 442, 109

- Laurent, P. & Titarchuk, L. 2007, *ApJ*, 656, 1056
- Lewin, W. H. G., van Paradijs, J., & van den Heuvel, E. P. J. 1995, *Cambridge Astrophysics Series*, Cambridge, MA: Cambridge University Press, —c1995, edited by Lewin, Walter H.G.; Van Paradijs, Jan; Van den Heuvel, Edward P.J.
- Makishima, K., Maejima, Y., Mitsuda, K., Bradt, H. V., Remillard, R. A., Tuohy, I. R., Hoshi, R., & Nakagawa, M. 1986, *ApJ*, 308, 635
- Miller, J. M. 2007, *ARA&A*, 45, 441
- Miller, M. C., Lamb, F. K., & Psaltis, D. 1998, *ApJ*, 508, 791
- Mitsuda, K., et al. 1984, *PASJ*, 36, 741
- Mitsuda, K., et al. 2007, *PASJ*, 59, 1
- Morrison, R., & McCammon, D. 1983, *ApJ*, 270, 119
- Nandra, K. et al. 1999, *ApJ*, 523, L17
- Nayakshin, S., Kazanas, D. & Kallman, T.R. 2000, *ApJ*, 537, 833
- Osherovich, V., & Titarchuk, L. 1999, *ApJ*, 522, L113
- Paizis, A., et al. 2006, *A&A*, 459, 187
- Reynolds, C.S. & Begelman, M.C. 1997, *ApJ*, 488, 109
- Smale, A. P. 1998, *ApJ*, 498, L141
- Smale, A. P., et al. 1993, *ApJ*, 410, 796
- Sobolev, V. V. 1957, *Soviet Astron.*, 1, 678
- Sunyaev, R. A., & Titarchuk, L. G. 1980, *A&A*, 86, 121
- Titarchuk, L. 1994, *ApJ*, 434, 570
- Titarchuk, L. 2002, *ApJ*, 578, L71 .
- Titarchuk, L., & Shaposhnikov, N. 2002, *ApJ*, 570, L25
- Titarchuk, L., Kuznetsov, S., & Shaposhnikov, N. 2007, *ApJ*, 667, 404
- Titarchuk, L.G., Osherovich, V.A. & Kuznetsov, S.I. 1999, *ApJ*, 525, L129

Titarchuk, L., Shaposhnikov, N. & Arefiev, V. 2007, ApJ, 660, 556

Titarchuk, L. & Wood, K. 2002, ApJ, 577, L23

Wijnands, R., et al. 1998, ApJ, 493, L87

Table 1. Best-fit Parameters for the *Suzaku* Spectrum of Cygnus X-2

Parameter	Model 1 ^a	Model 2 ^b	Model 3 ^c	Model 4 ^d
N_H , cm ²	0.273±0.002	0.274±0.002	0.275±0.002	0.273±0.03
T_{in} , keV	1.2±0.1	1.17±0.09	1.18±0.09	1.16±0.07
T_0 , keV	0.85±0.08	0.89±0.06	0.91±0.07	0.82±0.05
kT_e , keV	2.48±0.04	2.48±0.03	2.49±0.04	2.48±0.03
τ_p	19.2±3.7	18.5±2.8	18.6±3.2	19.2±2.2
E_L , keV	5.90±0.69	6.96±0.17	6.94±0.14	6.92±0.04
σ , keV	0.81±0.09	-	-	-
β_L	-	7.05±2.17	4.17±0.17	-
R_{in} , R_G	-	8.09±0.62	7.17±0.18	-
i_L , deg	-	24.8±1.7	24.8±0.8	-
τ_w	-	-	-	3.88±0.10
v/c , 10 ⁻³	-	-	-	7.7±1.1
kT_w , keV	-	-	-	0.20±0.05
EW_L , eV	68±19	66±11	65±9	160±31
χ^2/N_{dof}	492.5/335	425.9/333	429.2/333	410.1/333

^aXSPEC Model: `wabs(comptt+diskbb+gaussian)`

^bXSPEC Model: `wabs(comptt+diskbb+diskbb)`

^cXSPEC Model: `wabs(comptt+diskbb+laor)`

^dXSPEC Model: `wabs(comptt+diskbb+windline)`

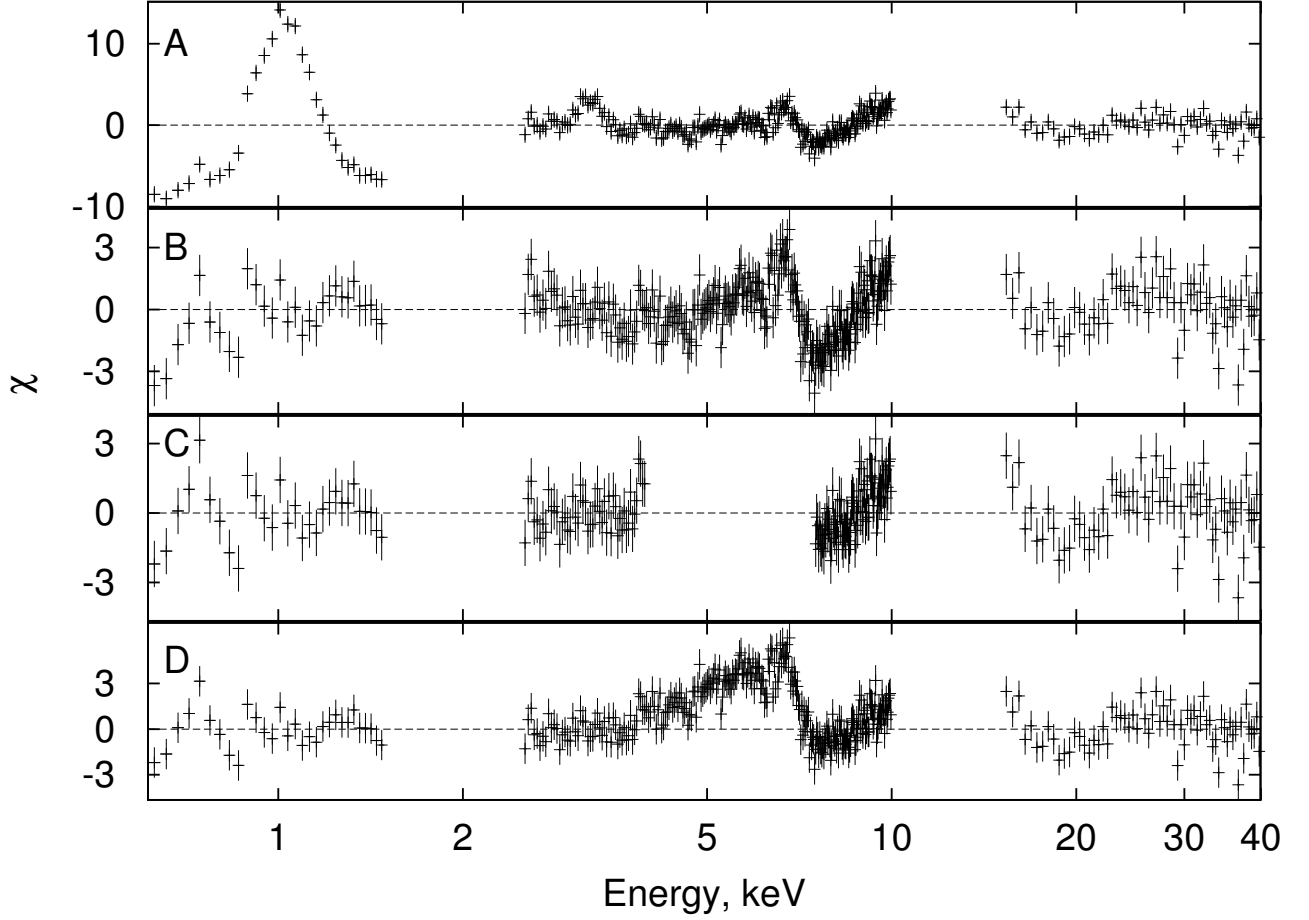


Fig. 1.— Identification of the continuum model and narrow lines in the *Suzaku* spectrum of Cygnus X-2. A) Fit with continuum model `wabs(comptt+diskbb)` only. B) Fit with lines added at 1 keV and 3.2 keV. C) Fit with energy range from 4.0 keV to 7.5 keV excluded. D) Residuals for the model obtained in C) with channels between 4.0 keV and 7.5 keV noticed. Strongly red-skewed line is apparent. See text for details.

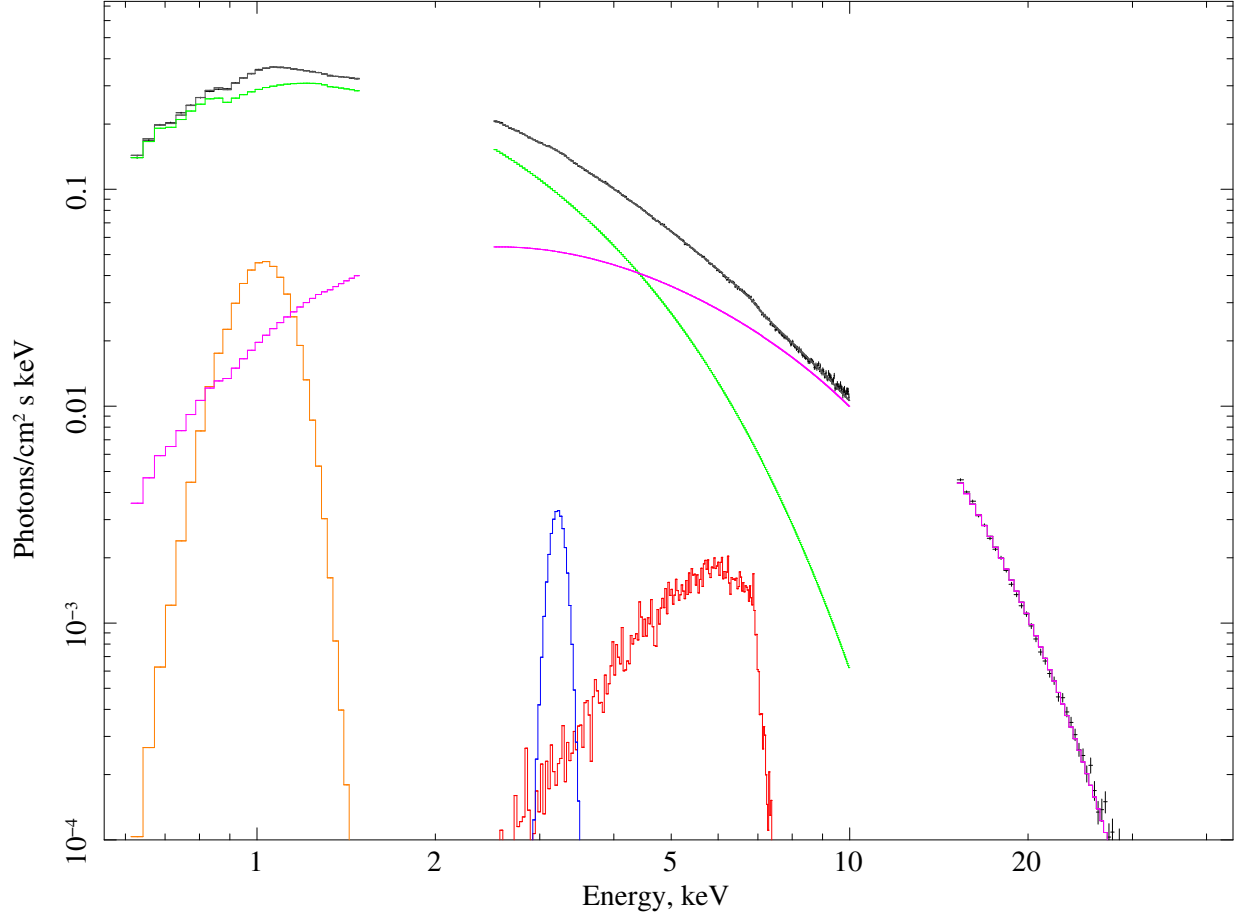


Fig. 2.— Unfolded model fit to the *Suzaku* Cyg X-2 spectrum with the Model 4. The best-fit model of the source spectrum consist of `comptt` (magenta), `diskbb` (green), `windline` (red) and two `gaussians` at 1 keV (brown) and 3.2 keV (blue).

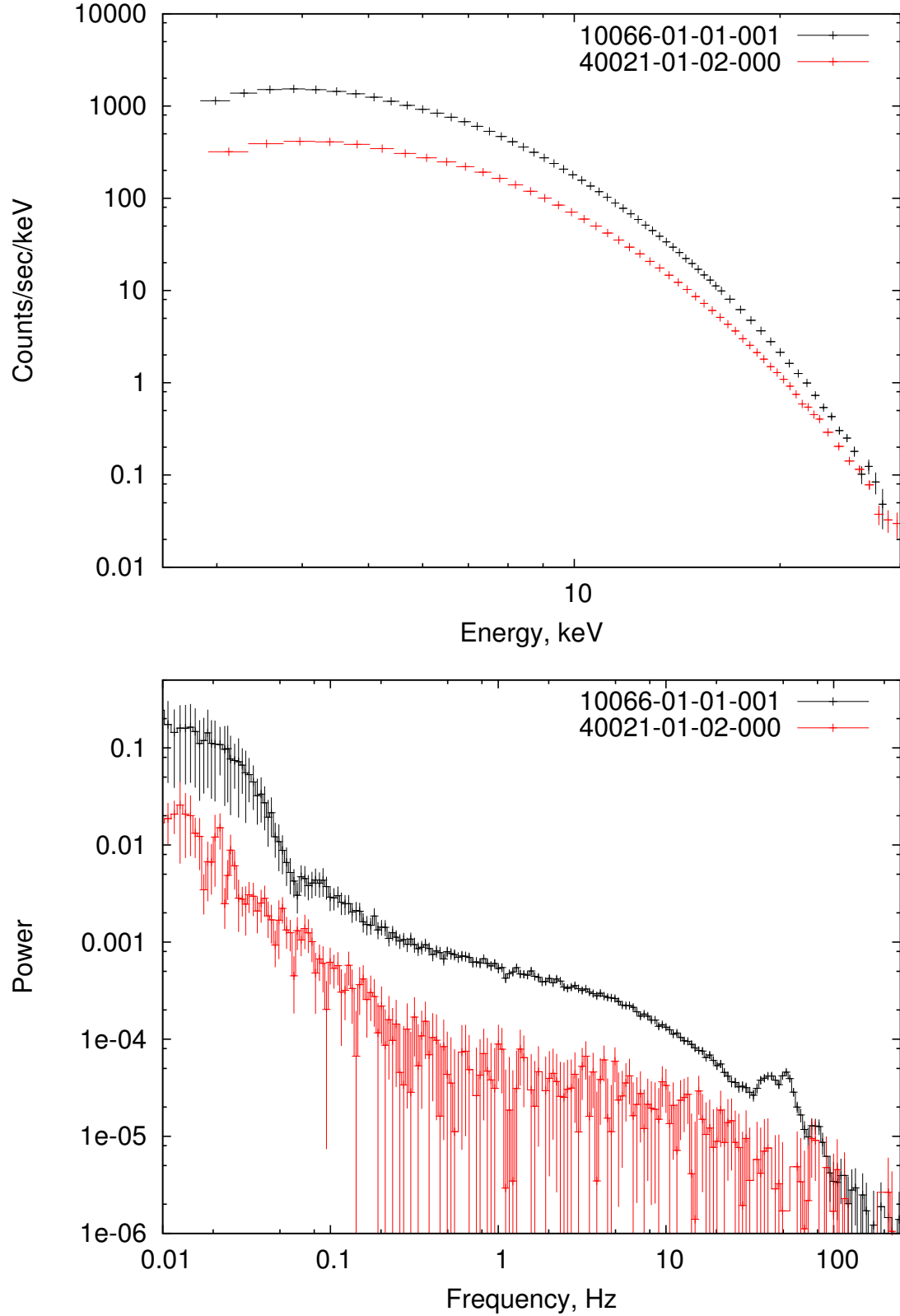


Fig. 3.— Energy and Power Density spectra as observed by *RXTE* during observation 10066-01-01-001 (black) and 40021-01-02-000 (red). Spectral parameters during observation 40021-01-02-000 are similar to those measured during *Suzaku* observation. Timing analysis shows that high frequency variability during this particular observation is strongly suppressed.